TÜBİTAK

Turkish Journal of Physics

http://journals.tubitak.gov.tr/physics/

Research Article

Turk J Phys
(2016) 40: 287 – 296

doi:10.3906/fiz-1604-3

Effect of glow discharge plasma on step index polymer optical fiber parameters

Mohamed MEDHAT[1], El-Sayed EL-ZAIAT[1,*], Mohamed SAUDY[1], Mona OMAR[1], Hassanein SHABAN[2]

[1]Department of Physics, Faculty of Science, Ain Shams University, Abbasia, Cairo, Egypt
[2]Department of Basic Science, Faculty of Engineering, The British University in Egypt, El Sherouk City, Cairo, Egypt

Received: 04.04.2016 • **Accepted/Published Online:** 06.06.2016 • **Final Version:** 01.12.2016

Abstract: DC glow discharge plasma of power 40 W was applied to step index polymer optical fibers for different exposure times. Nitrogen, oxygen, and hydrogen gases were used to obtain the glow discharge. The fiber core material was poly methyl methacrylate and the cladding was fluorinated polymer. The effect of plasma on the optical parameters, such as core index profile, cladding index, and the numerical aperture, was studied by multiple beam interference fringes and Fourier transformation of infrared spectroscopy spectra. It was found that the plasma treatment affected the optical parameters of both the cladding and the core regions of optical fibers. The optical parameters also changed with the treatment time. The hydrogen plasma had effects greater than those of nitrogen and oxygen plasma. These observed results can be explained by the effect of the electric field during plasma treatment. The studied optical fibers after plasma treatment can be used as inverted-graded index with its important applications.

Key words: Glow discharge plasma, multiple beam interference fringes, polymer fiber

1. Introduction

Optical fibers are a dielectric transparent medium that conducts and guides light. They have many civilian and military applications in different fields of our everyday life [1]. There are many classifications of optical fibers depending on the fiber material (glass or polymer), way of signal propagation, and the fiber diameter (single mode or multimode), as well as depending on the relation between the fiber's refractive indices versus the fiber radius, which is called the index profile (step index or graded index) [2].

Glass fibers are preferable for long distances of hundreds of kilometers. However, they suffer from difficulty of handling and the need for a long time for training [3]. Polymer optical fibers (POFs) have more advantages such as low cost, large numerical aperture, and suitable flexibility that give them priority for short distances of hundreds of meters [4]. In addition, POFs can be stretched further without breaking; a high refractive index difference is maintained between core and cladding, and hence high numerical aperture [5].

Poly methyl methacrylate (PMMA) shows the best optical properties among transparent polymers, being a very common core material in polymeric optical fibers, waveguides, and optical interconnects [5]. Thus, the use of polymers has been considered due to the intrinsic versatility molecular structure that allows advantageous refractive index modeling for core and cladding, and also due to their easy fabrication process or patterning capability [6]. Low refractive index is a requirement for cladding material, and it is usually achieved

*Correspondence: syelzaiat@hotmail.com

with fluorinated polymers [7]. Multiple beam interference fringes (MBFs) in transmission have been used to investigate the surface topography of surfaces and to measure the thickness of thin films. MBFs formed across a fiber material when immersed in a wedge interferometer illuminated by a parallel beam of monochromatic light have been used to measure the refractive index and birefringence of fibers. These fringes have also been used to examine the layer structure of graded index materials. Optical interferometry is one of the most important accurate methods for characterization of fiber parameters [8].

Plasma is known as an ionized gas, and consists of species electrons, ions, and neutral particles. These energetic particles have high activity [9]. Plasma treatment is a field for processing of many materials, especially in the polymer field. Plasma processing has been widely used in a large number of technologies [10]. Glow discharge plasma gives excellent results in the surface modification of materials and industrial components [11].

In the present work, the effects of nitrogen, oxygen, and hydrogen glow discharge plasmas on step-index polymer fiber samples were investigated. The fiber core material was PMMA and the cladding was fluorinated polymer. The optical fibers were exposed to nitrogen, oxygen, and hydrogen plasmas at different exposure times. Multiple beam interference fringes were applied to detect the variation in some optical parameters associated with optical fibers. FTIR spectroscopy was applied to unexposed and exposed samples of the fibers to make a diagnostic interpretation of the changes in the structure of the samples after exposure to plasmas. The observed results are explained by the effect of the electric field during the plasma treatment.

2. Experimental work

2.1. Fiber material

The fiber sample had a core material of PMMA and the cladding material was fluorinated polymer. The chemical structure is shown in Figure 1. PMMA is produced from ethylene, hydrocyanic acid, and methyl alcohol. It is resistant to water, dyes, diluted acids, petrol, mineral oil, and turpentine oil. Furthermore, it is a polymerized material that has an amorphous structure. The Table shows the specifications of the polymer fibers used.

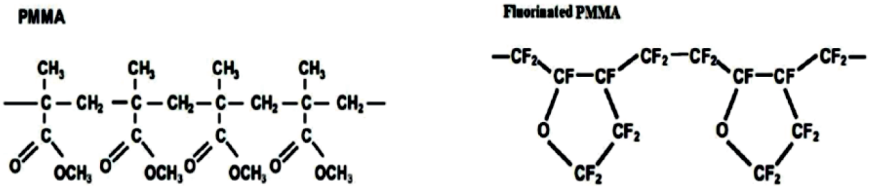

Figure 1. The chemical structure of the step index optical fiber used.

Table. Specifications of the polymer optical fiber sample used.

Core material	PMMA
Core diameter	240 ± 23 μm
Core refractive index	1.49
Cladding material	Fluorinated polymer
Cladding diameter	250 ± 23 μm
Numerical aperture	0.5

2.2. Plasma exposure

A plasma discharge setup was used for irradiating the polymer optical fibers. Figure 2a shows the schematic diagram of the plasma discharge setup used for irradiating the polymer optical fibers. Figure 2b shows a

photograph of the plasma produced. The setup consists of three main parts: vacuum system, pseudodischarge tube, and power supply circuit [12]. Continuous gas flow through the discharge vessel is maintained to sweep out the impurities from the system; the flow of the gas is controlled by a needle valve and hence adjusting the working gas pressure inside the gas tube. The vessel of the cell is made of cylindrical Pyrex glass about 10 cm in diameter and 25 cm long. The cathode is a copper rod of 5 cm diameter, which is inserted in the Pyrex glass. The anode is steel mesh 30 holes/inch^2 and placed 3 mm from the cathode. The electrodes are fixed in the cell by two flanges. The tube should be evacuated and filled with the working gas at the required pressure $\boldsymbol{p}$. Then a sufficiently high voltage is applied across the two electrodes until a discharge current flows, which means that an electrical breakdown occurs. The expansion plasma is generated outside the two electrodes. This is clear, since the electrode separation distance is less than or equal to the mean free path of the electrons.

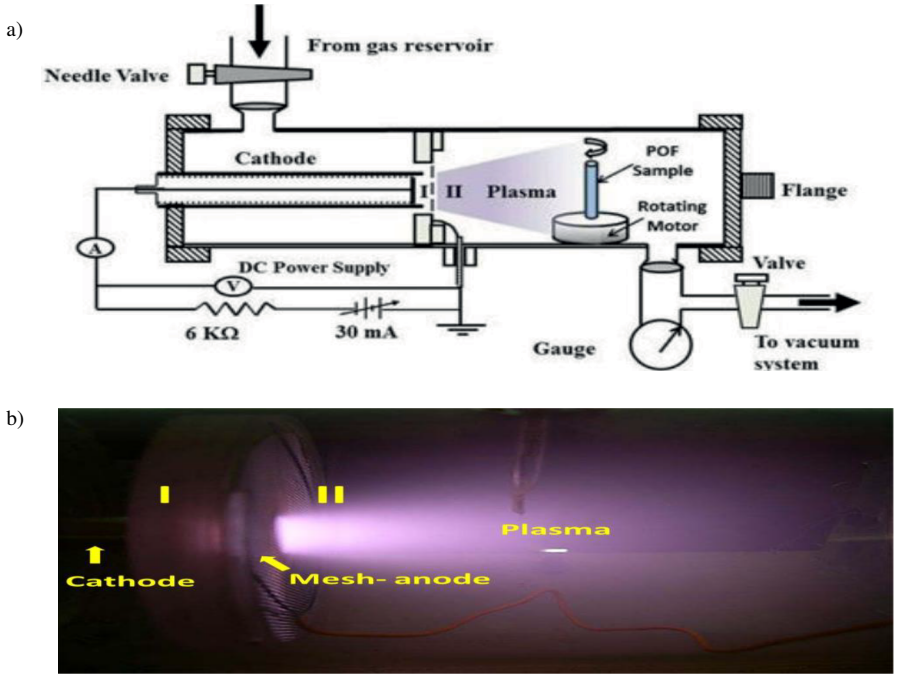

Figure 2. a) Schematic diagram of the discharge experiment arrangement. b) Photograph of the plasma in the discharge experiment arrangement.

The fiber sample was held in the plasma region and rotated over a small motor inserted in the plasma tube 5 cm from the anode for different exposure times. The appropriate values of the pressure p and the current intensity were 0.4 Torr and 30 mA, respectively. Nitrogen, oxygen, and hydrogen gases were used for treatment of polymer optical fibers.

2.3. Optical setup

Multiple beam interference was used to show the shape of interference fringes inside the fiber material [13]. The interferometric investigation was done by inserting the fiber material in a wedge interferometer with the fiber axis perpendicular to the edge of the wedge [13]. A schematic diagram of the optical setup is shown in Figure 3a and a photograph of it is shown in Figure 3b. It consists of a mercury lamp, s, as a light source followed by a condensing lens, L1, which forms a diminished intense image of the source on the diaphragm, D, which is

located at the focus of the collimating lens, L2, which allows a parallel light to pass through the mercury green filter, F, and being reflected by mirror, M, to fall normally on the interferometer, I, which is at the object plane of the microscope. Thus, fiber being immersed in a silvered liquid wedge interferometer is illuminated by a parallel monochromatic beam of light of wavelength $\lambda = 5461$ Å. The screws of the wedge interferometer were adjusted to secure the interference fringes in the liquid region being normal to the fiber axis. The shape and magnitude of the fringe shift across the fiber depend on the relative values of refractive indices of the immersion liquid, cladding, and core of the fiber used.

a)

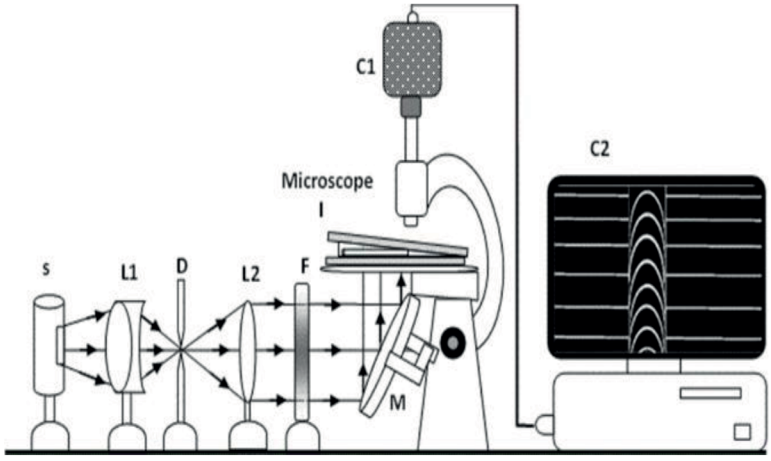

b)

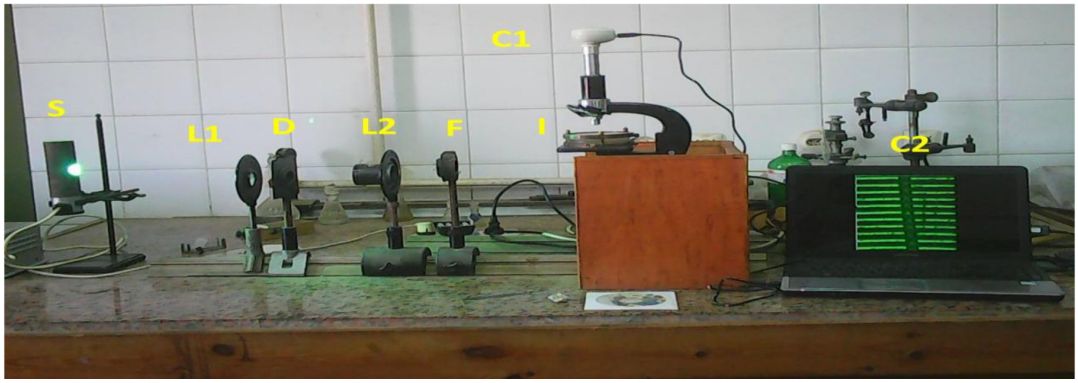

Figure 3. a) Optical setup for producing multiple-beam Fizeau fringes in transmission. s, Mercury lamp; L_1, condensing lens; D, iris diaphragm; L_2, collimating lens; F, monochromatic filter, M, reflecting mirror of microscope; I, silvered liquid wedge interferometer; C_1, a camera attached to the microscope; C_2, computer. b) Photograph of the optical setup for producing multiple-beam Fizeau fringes.

3. Results and discussion

3.1. FTIR spectroscopy

To characterize the chemical structure of the modified optical fiber, Figure 4 shows FTIR spectra of an unexposed fiber sample, and nitrogen, oxygen, and hydrogen plasma exposed fiber samples. FTIR spectra of the samples show similar bonds except for some changes due to plasma treatment. It can be seen in Figure 4 that after

treatment with nitrogen, oxygen, and hydrogen plasma, transmission of the band corresponding to CH and C=O at 3000 and 1695 cm^{-1}, respectively, increased relatively. The OH peak transmission bond at 3400 cm^{-1} for oxygen and nitrogen increased relatively while the transmission of OH bonds for hydrogen decreased [14,15]. The spectra of the samples exposed to nitrogen and oxygen were measured after 6 min of exposure, while the maximum hydrogen exposure time was 150 s. It is important to mention that increasing exposure time to hydrogen leads to burning of the fiber samples.

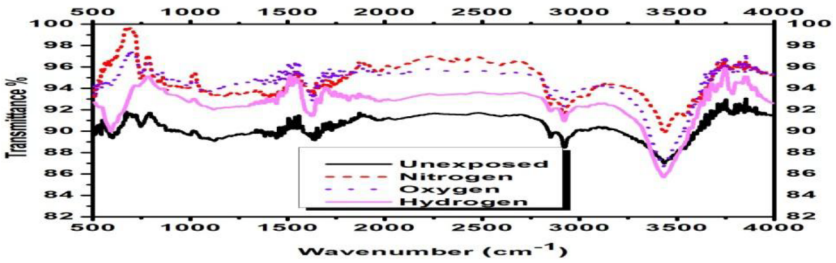

Figure 4. FTIR of polymer fiber samples.

3.2. Variations in cladding index

The cladding of the fiber is fluorinated polymer. Figure 5 shows the variation in the cladding refractive index of the fiber with nitrogen, oxygen, and hydrogen plasma exposure at different times. It can be seen that a slight increase occurred in the refractive index upon exposure to oxygen and nitrogen plasma. On the other hand, the hydrogen plasma decreased the refractive index of the cladding fiber. This may be explained by different effects and reactivity of the plasma species of different gases on the cladding fiber [16].

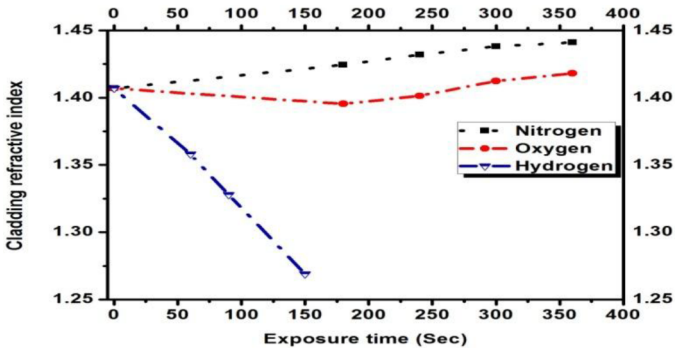

Figure 5. Variations in the cladding index with plasma exposure times for different gases.

3.3. Variations in core index profile

Figure 6 shows the variation in the core refractive index profile with nitrogen plasma exposure time. It indicates that there was a regular increase in the peripheral core index with increasing plasma exposure time. The index variation decreased as we moved toward the center of the fiber. There was near equality between the core index profiles at exposure times (3, 5, and 6 min) and a noticeable increase in time (4 min). Figure 7 shows the variation in the core refractive index profile with oxygen plasma exposure time. The core index variation decreased as we moved toward the center of the fiber. The core index profiles at exposure time 180 s had the greatest value and at 300 s the core index profile had the lowest value compared to the other exposure times. Figure 8 shows the variation in the core refractive index profile with hydrogen plasma exposure time. It

indicates that there was a regular increase in the core index with increasing plasma exposure time. This index variation decreased as we moved toward the center of the fiber.

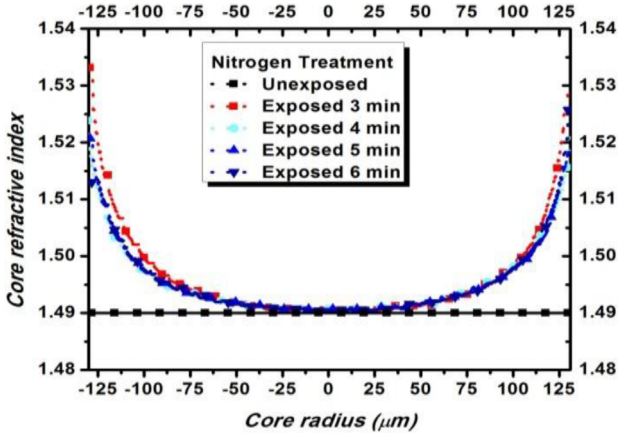

Figure 6. The core index profile variation with nitrogen plasma at different exposure times.

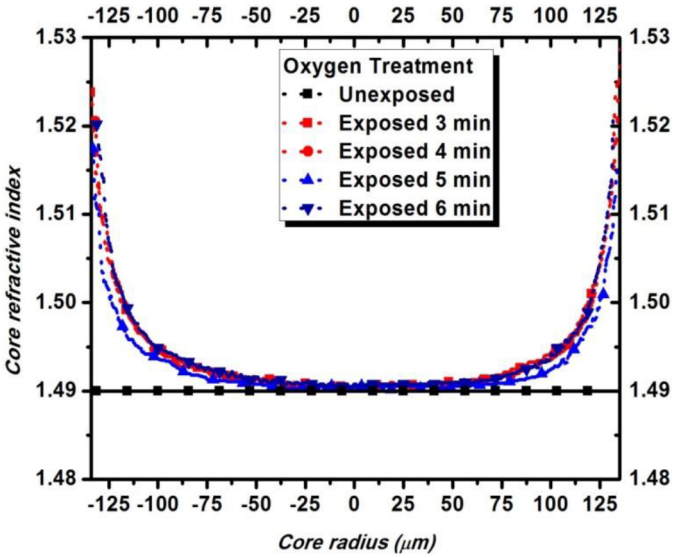

Figure 7. The core index profile variation with oxygen plasma at different exposure times.

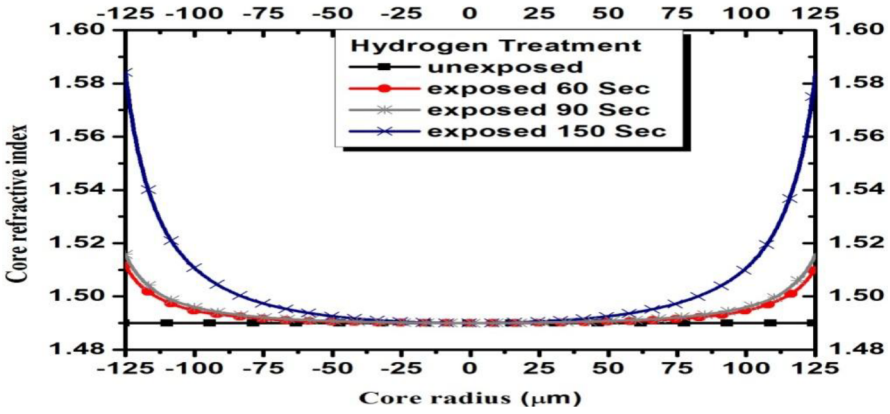

Figure 8. The core index profile variation with hydrogen plasma at different exposure times.

In Figures 6–8, it is shown that the hydrogen plasma had more effect than nitrogen and oxygen. This appears in the increase in the refractive index of the core after exposure to hydrogen plasma. This can be explained by the increase in C–H bonds, which increases the refractive index. The increase in C–H bonds can lead to the formation of some functional group at the surface of the core. Thus, the plasma treatment of a step-index fiber can convert it to an inverted-graded index (IGI) fiber [17].

3.4. Affected core depth due to plasma exposure

Figure 9 shows the affected depth in the core region with nitrogen, oxygen, and hydrogen plasma exposure times. It is indicated that there was a regular increase in the peripheral core index with increasing exposure time. The hydrogen plasma had a more affected core depth than nitrogen and oxygen plasma. This is because hydrogen is a more active gas and has a lower mass than nitrogen and oxygen.

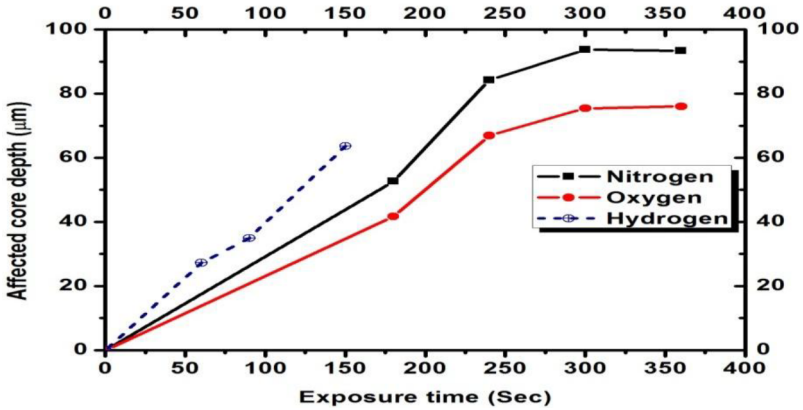

Figure 9. The affected depth in the core region with exposure times for different gases.

3.5. Numerical aperture (N.A.)

The numerical aperture is calculated according to Eq. (1). Since the refractive index of the core center is constant but the cladding refractive index is changed, it is indicated that there was a change in the numerical aperture with increasing exposure time.

$$N.A. = \sqrt{n_c^2 - n_{cl}^2} \tag{1}$$

The numerical aperture variation at different plasma gas exposure times is shown in Figure 10. It is indicated that there was a slight decrease in the numerical aperture with increasing exposure time for nitrogen and oxygen plasma. This behavior is due to the increase in the cladding refractive index with plasma exposure. For hydrogen plasma, there was an obvious increase in the numerical aperture with increasing exposure time.

3.6. Maximum variation in core index

The maximum value of the core refractive index was located at the core–cladding interface. Moreover, the core refractive index at the core–cladding interface increased with increasing plasma exposure time. Figure 11 shows the maximum core refractive index variation for the nitrogen, oxygen, and hydrogen plasma exposure times. The maximum core refractive index increased linearly with the nitrogen and oxygen plasma exposure times until 240 s, and then followed a stationary condition, indicating stopping of additional interaction. For hydrogen, the maximum value of the core refractive index located at the core–cladding interface increased with the increasing

plasma exposure time. This behavior variation of different plasma gases may find some useful applications in technology.

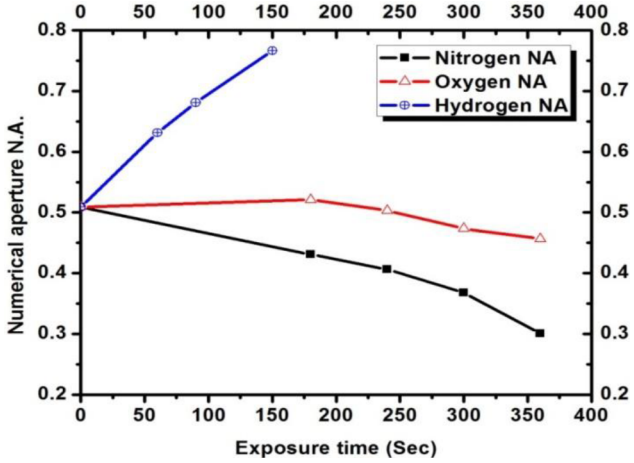

Figure 10. Variation in the numerical aperture with exposure times for different gases.

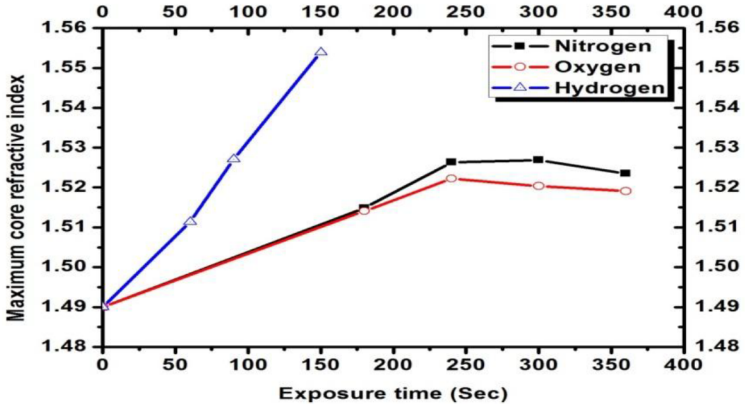

Figure 11. Maximum core refractive index variation with exposure times for different gases.

4. Discussion

It has been proved that plasma treatment creates polar surface functional groups such as carbonyl, carboxyl groups, and nitrogen oxide compounds on the fiber sample surface. These changes produce a higher surface polarity of plasma treated samples as compared to untreated ones. This can be used to explain the experimentally observed higher values of the surface refractive index of the fiber cladding. Most of the electric charges are deposited on the fiber surface and only a small part of charges can pass into a certain depth of the fiber. The greater is the value of the grid potential during plasma treatment, the bigger is the value of that constant electric field that affects the fiber sample.

Plasma treatment would cause an additional polarizability, ΔP. This produces an increase in the fiber refractive index. Using the Lorentz–Lorenz relation, the following approximation can be written for the change in the refractive index [18]:

$$\Delta n = \left(\frac{n^2+2}{3}\right)^2 \frac{N_M \Delta P}{2 \in_0} \tag{2}$$

where $\in_0$ is the permittivity, n is the refractive index, and N_m is the number of molecules per unit volume.

The effect of plasma on the fiber sample can be explained as the effect of the electric field associated with the potential difference during the exposure to plasma. Applications of the electric field on the fiber sample lead to an increase in the refractive index due to the increase in polarizability such that [19]

$$\Delta P = \frac{(n^2-1)\Delta E}{4\pi} \tag{3}$$

The electric fields used were 629.29, 417.28, and 283.14 V/m with hydrogen, nitrogen, and oxygen plasma, respectively. Thus hydrogen plasma had effects greater than those of nitrogen and oxygen plasma.

It should be noted that, during the plasma treatment, there was an effect of the heat on the fiber material. The thermo-optic constant of PMMA was negative (-1×10^{-4} K^{-1}) and a very small decrease in the refractive index was produced.

5. Conclusion

Plasma treatment was applied to step-index polymer optical fiber samples for different exposure times. The fiber samples were investigated by using multiple beam interference fringes. It is found that the plasma treatment had an observed effect on the optical parameters of the cladding and the core regions of polymer optical fibers. The method of MBFs in transmission is a sensitive method for investigating the effect of plasma on the parameters of the polymer fiber. Optical interferometry is a more sensitive tool for detecting smaller variations in the refractive index along each point of the fiber diameter than FTIR spectroscopy.

Hydrogen plasma was more interactive with a fluorinated layer on the optical fiber. In the case of oxygen and nitrogen, the variation was small. The core refractive index increased with increasing plasma exposure time. The core index variation decreased upon moving toward the center due to the decrease in plasma species penetration. A mechanism based on the effect of the electric field during plasma exposure was used for interpretation of the results of the plasma treatment. The electric fields used were 629.29, 417.28, and 283.14 V/m with hydrogen, nitrogen, and oxygen plasma, respectively. Thus hydrogen plasma had effects greater than those of nitrogen and oxygen plasma.

The plasma treatment of the step index fluorinated PMMA polymer fiber converts it to inverted-graded index (IGI), which has wide technological applications via the advantage of the sensitivity of the IGI fibers to refractive index variations.

References

[1] Personick, S. D. *Fiber Optics: Technology and Applications*; Springer: New York, NY, USA, 1985.

[2] Bailey, D.; Wright, E. *Practical Fiber Optics*; Newnes: Oxford, UK, 2003.

[3] DeCusatis, C.; DeCusatis, C. J. S. *Fiber Optic Essentials*; Elsevier/Academic Press: San Diego, CA, USA, 2005.

[4] Murata, H. *Handbook of Optical Fibers and Cables*, 2nd ed; Marcel Dekker Inc.: New York, NY, USA, 1996.

[5] Koike, K.; Koike, Y. *J. Lightwave Technol.* **2009**, *27*, 4-46.

[6] Park, S.; Cho, K.; Gi-Choi, C. *J. Colloid Interf. Sci.* **2003**, *258*, 424-426.

[7] Padilha, G. S.; Giacon, V. M.; Bartoli, J. R. *Polimeros* **2013**, *23*, 585-589.

[8] Barakat, N.; El-Hennawi, H. A.; El-Zaiat, S. Y.; Hassan, R. *Pure Appl. Opt.* **1996**, *5*, 27-34.

[9] El-Nagar, K.; Saudy, M. A.; Eatah, A. I.; Masoud, M. M. *J. Text. I.* **2006**, *97*, 111-117.

[10] Grill, A. *Cold Plasma Materials Fabrication: From Fundamentals to Applications*, 1st ed, IEEE Press: New York, NY, USA, 1994.

[11] Luo, H. L.; Sheng, J.; Wan, Y. Z. *Appl. Surf. Sci.* **2007**, *253*, 5203-5207.

[12] Saudy, M. A. *Plasma Devices and Operations* **2009**, *17*, 88-96.

[13] Barakat, N.; Hamza, A. A. *Interferometry of Fibrous Material*; Adam Hilger: Bristol, UK, 1990.

[14] Steiner, T. *Chem. Comm.* **1997**, *8*, 727-734.

[15] Silverstein, M. R.; Webster, X. F.; Kiemle, D. J. *Spectrometric Identification of Organic Compounds*; New York, NY, USA: John Wiley & Sons, 2005.

[16] Ando, S. *J. Photopolymer Sci. Tech.* **2004**, *17*, 219-232.

[17] Matehec, V.; Chomat, M.; Kasik, I.; Ctyroky, J.; Berkova, D.; Hayer, M. *Sensors and Actuators B*, **1998**, *51*, 340-347.

[18] Yovcheva, T.; Babeva, Tz.; Nikkolova, K.; Mekishev, K. *J. Opt. A: Pure Appl. Opt.* **2008**, *10*, 055008 (4pp).

[19] Konsin, P.; Sorkin, B. *Physica B* **2015**, *478*, 131-134.